Platinum(II) Phosphido Complexes as Metalloligands. Structural and Spectroscopic Consequences of Conversion from Terminal to Bridging Coordination

Corina Scriban,[†] Denyce K. Wicht,[†,‡] David S. Glueck,*[,†] Lev N. Zakharov,[§] James A. Golen,[§] and Arnold L. Rheingold[§]

6128 Burke Laboratory, Department of Chemistry, Dartmouth College, Hanover, New Hampshire 03755, and Department of Chemistry and Biochemistry, University of California, San Diego, 9500 Gilman Drive, La Jolla, California 92093

Received March 2, 2005

Treatment of the terminal phosphido complexes Pt(dppe)(Me)(PPh(R)) (R = Ph (**1**), *i*-Bu (**6**)) with Pt(dppe)(Me)(OTf) gave the cationic μ-phosphido complexes [(Pt(dppe)(Me))$_2$(μ-PPh(R))][OTf] (R = Ph (**7**), *i*-Bu (**8**)). Similarly, Pt((*R*,*R*)-Me-Duphos)(Me)(PPh(*i*-Bu)) (**10**) was converted to [(Pt((*R*,*R*)-Me-Duphos)(Me))$_2$(μ-PPh(*i*-Bu))][OTf] (**11**). A fluxional process in **8** and **11**, presumably involving hindered rotation about the Pt−PPh(*i*-Bu) bonds, was observed by NMR spectroscopy; it resulted in two diastereomers for **8** and four for **11** at low temperature. Coordination of the metalloligand **10** to the [Pt((*R*,*R*)-Me-Duphos)(Me)]$^+$ fragment, yielding **11**, resulted in structural changes at the Pt−phosphido group, whose geometry changed from distorted pyramidal to tetrahedral. Decomposition of **6** also gave the cation **8**, while oxidation of **6** with H_2O_2 gave the crystallographically characterized phosphido oxide complex Pt(dppe)(Me)(P(O)Ph(*i*-Bu)) (**12**).

Introduction

Forty years ago, Chatt and Davidson considered the possibility of terminal Pt−PPh_2 ligands: "it seems unlikely that they can exist in the Pt(II) series except under very special circumstances, the tendency to occupy bridging positions between Pt atoms being too strong."[1] Avoiding labile ligands such as halides and monodentate phosphines is one way to fulfill the required special circumstances and prepare stable Pt(II) terminal phosphido complexes, such as the ones shown in Chart 1.[2]

Chart 1. Pt(II) Terminal Phosphido Complexes 1−4 and Dinuclear μ-Phosphido Complex 5 Formed When 3 Acts as a Ligand[3]

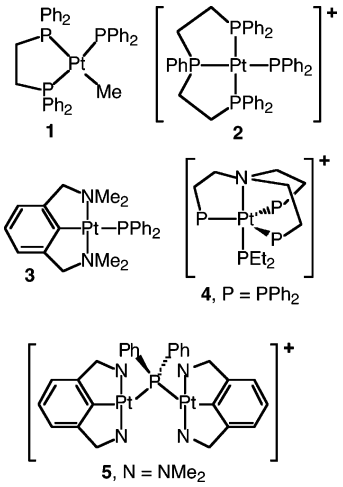

Such metal phosphido complexes contain pyramidal, nucleophilic phosphorus centers, which can act as ligands to other metals.[4] For example, the reaction of **3** with [Pt(NCN)(H_2O)]$^+$ (NCN = 2,6-(CH_2NMe_2)$_2$$C_6H_3$) gave the bimetallic complex **5**.[3c] We report here that Pt phosphido compounds such as **1** can also be converted into analogous μ-phosphido complexes, and we describe the spectroscopic and structural consequences of this change in coordination mode.

* To whom correspondence should be addressed. E-mail: glueck@dartmouth.edu.

[†] Dartmouth College.

[‡] Present address: Department of Chemistry, Suffolk University, Boston, Massachusetts 02108.

[§] University of California, San Diego.

(1) Chatt, J.; Davidson, J. M. *J. Chem. Soc.* **1964**, 2433−2445.

(2) For other terminal Pt−phosphido complexes, see: (a) Allen, C. W.; Ebsworth, E. A. V.; Henderson, S. G.; Rankin, D. W. H.; Robertson, H. E.; Turner, B.; Whitelock, J. D. *J. Chem. Soc., Dalton Trans.* **1986**, 1333−1338. (b) Schaefer, H.; Binder, D. *Z. Anorg. Allg. Chem.* **1988**, *560*, 65−79. (c) Mastrorilli, P.; Nobile, C. F.; Fanizzi, F. P.; Latronico, M.; Hu, C.; Englert, U. *Eur. J. Inorg. Chem.* **2002**, 1210−1218. (d) Zhuravel, M. A.; Glueck, D. S.; Zakharov, L. N.; Rheingold, A. L. *Organometallics* **2002**, *21*, 3208−3214. (e) Kovacik, I.; Wicht, D. K.; Grewal, N. S.; Glueck, D. S.; Incarvito, C. D.; Guzei, I. A.; Rheingold, A. L. *Organometallics* **2000**, *19*, 950−953. (f) Wicht, D. K.; Kourkine, I. V.; Kovacik, I.; Glueck, D. S.; Concolino, T. E.; Yap, G. P. A.; Incarvito, C. D.; Rheingold, A. L. *Organometallics* **1999**, *18*, 5381−5394. (g) Wicht, D. K.; Glueck, D. S.; Liable-Sands, L. M.; Rheingold, A. L. *Organometallics* **1999**, *18*, 5130−5140. (h) Wicht, D. K.; Kovacik, I.; Glueck, D. S.; Liable-Sands, L. M.; Incarvito, C. D.; Rheingold, A. L. *Organometallics* **1999**, *18*, 5141−5151. (i) Kourkine, I. V.; Sargent, M. D.; Glueck, D. S. *Organometallics* **1998**, *17*, 125−127. (j) Wicht, D. K.; Kourkine, I. V.; Lew, B. M.; Nthenge, J. M.; Glueck, D. S. *J. Am. Chem. Soc.* **1997**, *119*, 5039−5040. (k) David, M.-A.; Wicht, D. K.; Glueck, D. S.; Yap, G. P. A.; Liable-Sands, L. M.; Rheingold, A. L. *Organometallics* **1997**, *16*, 4768−4770. (l) David, M.-A.; Glueck, D. S.; Yap, G. P. A.; Rheingold, A. L. *Organometallics* **1995**, *14*, 4040−4042. (m) Scriban, C.; Glueck, D. S. *J. Am. Chem. Soc.* **2006**, *128*, 2788−2789. For a Pt−phosphenium complex, see: (n) Hardman, N. J.; Abrams, M. B.; Pribisko, M. A.; Gilbert, T. M.; Martin, R. L.; Kubas, G. J.; Baker, R. T. *Angew. Chem., Int. Ed.* **2004**, *43*, 1955−1958.

(3) For **1**, see: (a) Wicht, D. K.; Paisner, S. N.; Lew, B. M.; Glueck, D. S.; Yap, G. P. A.; Liable-Sands, L. M.; Rheingold, A. L.; Haar, C. M.; Nolan, S. P. *Organometallics* **1998**, *17*, 652−660. For **2**, see: (b) Handler, A.; Peringer, P.; Muller, E. P. *J. Chem. Soc., Dalton Trans.* **1990**, 3725−3727. For **3** and **5**, see: (c) Maassarani, F.; Davidson, M. F.; Wehman-Ooyevaar, I. C. M.; Grove, D. M.; van Koten, M. A.; Smeets, W. J. J.; Spek, A. L.; van Koten, G. *Inorg. Chim. Acta* **1995**, *235*, 327−338. For **4**, see: (d) Cecconi, F.; Ghilardi, C. A.; Midollini, S.; Moneti, S.; Orlandini, A.; Scapacci, G. *Inorg. Chim. Acta* **1991**, *189*, 105−110.

10.1021/om050149p CCC: $33.50
Publication on Web 06/09/2006

Scheme 1

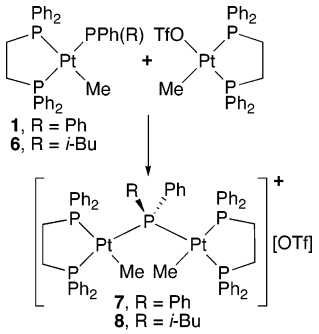

Scheme 2

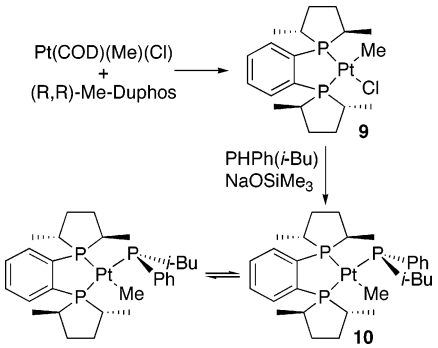

Results and Discussion

Synthesis of μ-Phosphido Complexes. In analogy to the formation of **5** from **3**, treatment of the terminal phosphido complexes **1** and Pt(dppe)(Me)(PPh(*i*-Bu)) (**6**)[3a] with Pt(dppe)(Me)(OTf),[5] generated from Pt(dppe)(Me)(Cl)[6] and AgOTf, gave the μ-phosphido complexes [(Pt(dppe)(Me))$_2$(μ-PPh(R))][OTf] (R = Ph (**7**), *i*-Bu (**8**); Scheme 1).

Analogous chiral μ-phosphido complexes were prepared using (*R,R*)-Me-Duphos instead of dppe. Treatment of Pt(COD)(Me)(Cl)[7] with (*R,R*)-Me-Duphos gave Pt((*R,R*)-Me-Duphos)(Me)(Cl) (**9**),[8] which was converted to the terminal phosphido complex Pt((*R,R*)-Me-Duphos)(Me)(PPh(*i*-Bu)) (**10**) by reaction with PHPh(*i*-Bu) in the presence of $NaOSiMe_3$ (Scheme 2).

The room-temperature NMR spectra of **10** were very broad, but at −40 °C, P inversion became slow on the NMR time scale and the expected two diastereomers could be observed, in a 1:1.2 ratio.[9] Measurement of the ^{31}P NMR coalescence temperatures for the phosphido P and the Duphos P trans to it (the cis Duphos P signal occurred at the same chemical shift for both diastereomers) provided the approximate free energy of activation for the fluxional process (Table 1),[10] with reasonable agreement between the data obtained for the two groups at different coalescence temperatures. The barrier to the dynamic process (a combination of P inversion and rotation about the Pt−P bond) of ca. 13 kcal/mol was similar to those we reported earlier for structurally analogous Pt−phosphido complexes.[2d,g,h]

Table 1. Variable-Temperature ^{31}P NMR Data (toluene-d_8) for Pt((*R,R*)-Me-Duphos)(Me)(PPh(*i*-Bu)) (10)[a]

resonance	δ (ppm)	$\Delta\nu$ (Hz)	T_c (K)	$\Delta G_c^{\ddagger}$
trans Duphos P	69.6, 67.8	809	283	12.8
PPh(*i*-Bu)	−57.3, −63.9	1350	313	13.4

[a] Chemical shifts and $\Delta\nu$ values were obtained from slow-exchange spectra at −60 °C. Estimated errors are different for each resonance; "typical" errors are 5 Hz in $\Delta\nu$, 10 °C in T_c, and 0.5 kcal/mol in $\Delta G_c^{\ddagger}$.

Scheme 3[a]

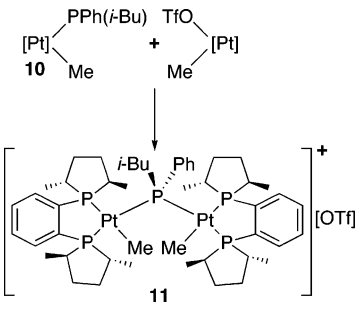

[a] [Pt] = Pt((*R,R*)-Me-Duphos.

As in the synthesis of phosphido-bridged complexes **7** and **8**, treatment of **9** with AgOTf, followed by reaction with **10**, gave [(Pt((*R,R*)-Me-Duphos)(Me))$_2$(μ-PPh(*i*-Bu))][OTf] (**11**) as a white solid which was soluble in polar solvents (Scheme 3).

NMR spectroscopy provided information on the structure and dynamics of the μ-phosphido complexes. Restricted rotation about the Pt−P bonds in complex **5** was proposed to account for its fluxionality.[3c] Similar processes are possible for **7**, **8**, and **11**. In the highest-symmetry complex, **7**, the bulky Pt(dppe)(Me) groups would be equivalent in conformations where they could be related by a C_2 axis (**A**) and/or a mirror plane containing the PPh_2 group (**B**). This would result in an AA′BB′X spin system for the isotopologue of **7** containing no ^{195}Pt atoms, along with AA′BB′XM and AA′BB′XMM′ spin systems for the other isotopologues.[11]

Because the unsymmetrical substitution of the phosphido group in **8** destroys the C_2 axis (**A** above), its Pt(dppe)(Me) groups can be equivalent only if they are related by a mirror plane (**B**) containing the PPh group and bisecting the P−CH_2-$CHMe_2$ moiety. This would give rise to spin systems such as those described above for **7**. However, if such a conformation is not accessible, the Pt(dppe)(Me) groups would be inequivalent, resulting in ABCDX and ABCDXMN spin systems for the isotopologues containing zero and two ^{195}Pt atoms. If the Pt nuclei are inequivalent, the isotopologues with one ^{195}Pt (ABCDXM spin systems) are different compounds, which should give rise to distinct ^{31}P NMR spectra. Finally, the chirality of (*R,R*)-Me-Duphos in **11** means that a potential mirror plane (**B**) cannot relate the Pt((*R,R*)-Me-Duphos)(Me) groups; therefore, this complex must display the reduced symmetry (ABCDX, etc.) described above.

The experimental NMR spectra were consistent with these predictions. For μ-PPh_2 complex **7**, ^{31}P and ^{1}H NMR spectra

(4) For some examples, see: (a) Carty, A. J.; MacLaughlin, S. A.; Nucciarone, D. In *Phosphorus-31 NMR Spectroscopy in Stereochemical Analysis*; Verkade, J. G., Quin, L. D., Eds.; VCH: Deerfield Beach, FL, 1987; pp 559−619. (b) Stephan, D. W. *Coord. Chem. Rev.* **1989**, *95*, 41−107. (c) Baker, R. T.; Tulip, T. H.; Wreford, S. S. *Inorg. Chem.* **1985**, *24*, 1379−1383. (d) Barre, C.; Boudot, P.; Kubicki, M. M.; Moise, C. *Inorg. Chem.* **1995**, *34*, 284−291.

(5) Hill, G. S.; Yap, G. P. A.; Puddephatt, R. J. *Organometallics* **1999**, *18*, 1408−1418.

(6) Appleton, T. G.; Bennett, M. A.; Tomkins, I. B. *J. Chem. Soc., Dalton Trans.* **1976**, 439−446.

(7) Clark, H. C.; Manzer, L. E. *J. Organomet. Chem.* **1973**, *59*, 411−428.

(8) For the analogous Pd complex, see: Murtuza, S.; Harkins, S. B.; Sen, A. *Macromolecules* **1999**, *32*, 8697−8702.

(9) Rogers, J. R.; Wagner, T. P. S.; Marynick, D. S. *Inorg. Chem.* **1994**, *33*, 3104−3110.

(10) Friebolin, H. *Basic One- and Two-Dimensional NMR Spectroscopy*, 2nd ed.; VCH: New York, 1993; pp 287−314.

(11) The spin system for the isotopologue with no ^{195}Pt could simplify to A_2B_2X if the dppe P nuclei are not magnetically inequivalent (for example, if the cis J_{PP}(dppe) value is 0). For the isotopologue with one ^{195}Pt, we assume that isotopic substitution does not change the ^{31}P NMR chemical shifts.

Table 2. $^{31}P\{^1H\}$ NMR Data for the Dinuclear Complexes [(Pt(diphos)(Me))$_2$(μ-PPh(R))][OTf] (7, 8, and 11)[a]

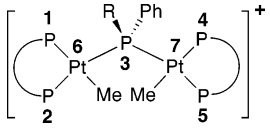

		δ (J_{Pt-P})						
diphos, R (no.)	temp (°C)	P_1	P_4	P_2	P_5	P_3	J_{23}, J_{53}	J_{13}, J_{43}
dppe, Ph (**7**)[b]	21	49.2 (1895)	49.2 (1895)	52.3 (2450)	52.3 (2450)	26.8 (2313)	341	16
dppe, *i*-Bu (**8**)[c]	21	48.5 (1906)	47.6 (1800)	52.8 (2338)	50.5 (2408)	1.0 (2289)	329, 352	15, 15
	−20	48.6 (1886)	47.2 (1863)	53.2[d] (2330)	50.4[e] (2405)	0.8 (2243, 2319)	337, 339	15, 15
	−40[f]	48.7 (1889)	47.0 (1864)	53.5 (2331)	50.4 (2405)	0.9 (2231, 2319)	334, 340	15, 15
	−40[f]	49.1 (1903)	47.4 (1883)	53.9 (2331)	50.7 (2405)	1.2[f]	334, 340	*f*
	100[g]	48.3 (1871)	48.3 (1871)	51.7 (2382)	51.7 (2382)	2.3 (2280)	338	15
Me-Duphos, *i*-Bu (**11**)	21[h]	69.3 (1840)	65.2 (1750)	67.5 (2292)	*h*	5.5 (2246)	334	*h*
		h	*h*	*h*	*h*	−7.1 (2307)	304	*h*
	100[i]	66.6 (1834)	65.6 (1801)	65.9 (2325)	65.8 (2330)	−2.1	340, 335	

[a] Chemical shift standard: external 85% H_3PO_4. Chemical shifts are given in ppm and coupling constants in Hz. Solvent: CD_2Cl_2 unless otherwise indicated. [b] Additional couplings for **7**: $J_{14} = 12$, $J_{25} = 5$, $J_{46} = J_{17} = 37$. [c] The signals were very broad; therefore, the expected two J_{Pt-P} couplings for P3 were not resolved. Although two different J_{P-P}(trans) couplings were observed from the dppe signals, the large line width means they are not significantly different. [d] $J_{12} = 6$. [e] $J_{45} = 4$. [f] Two diastereomers (7:1 ratio). Data for the major isomer are reported first. The breadth and lower intensity of the minor isomer signals prevented observation of the cis P−P couplings or J_{Pt-P} for the μ-PR_2 peak. [g] In DMSO-d_6. [h] Two diastereomers (2.5:1 ratio). Data for the major isomer are reported first. The signals were broad; only the μ-phosphido peak for the minor diastereomer **b** and one of the two expected trans Duphos signals for the major isomer **a** could be observed. [i] In 1,2-CD_2Cl_4; the peaks (especially the μ-phosphido signal) were broad.

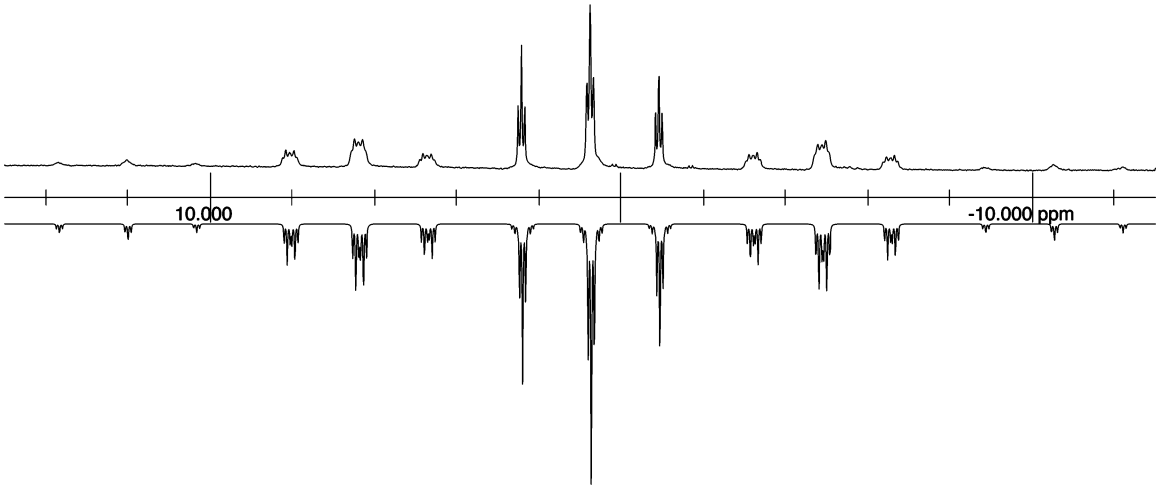

Figure 1. The μ-phosphido portion of the experimental (top) and simulated[13] (bottom) $^{31}P\{^1H\}$ NMR spectra of [(Pt(dppe)(Me))$_2$(μ-PPh(*i*-Bu))][OTf] (**8**) in CD_2Cl_2 at −20 °C.

indicated equivalent Pt(dppe)(Me) groups, even at low temperature. The ^{31}P NMR spectrum could be simulated with the parameters in Table 2 for the spin systems described above.[12,13]

The ^{31}P NMR spectrum of the μ-PPh(*i*-Bu) complex **8** was broadened at room temperature in CD_2Cl_2, but at −20 °C, sharp signals for the four different dppe P nuclei could be observed, consistent with inequivalent Pt(dppe)(Me) groups (Table 2). The μ-phosphido signal had an unusual appearance (Figure 1), since it showed two different large trans J_{PP} couplings (339 and 337 Hz) and two cis J_{PP} couplings of the same magnitude (15 Hz). Therefore, the central peak, which results from molecules which contain no ^{195}Pt, appeared as an overlapping doublet of doublets of triplets.

The two different Pt−P couplings to the μ-PR_2 group (2243 and 2319 Hz) can be seen most clearly in the major Pt satellite peaks, which are a superposition of subspectra of the two different isotopologues which contain one ^{195}Pt (ABCDXM spin systems). This effect explains why these peaks show a pattern distinct from that of the central signal, which is different from the usual observations in symmetrical dinuclear μ-phosphido complexes.[14] A second set of low-intensity satellite signals arises from the isotopologue which contains two ^{195}Pt nuclei. The $^1H\{^{31}P\}$ NMR spectrum of **8** at 25 °C showed only broad signals, but the resonances were much sharper at −60 °C, and two different Pt−Me signals were observed at δ 1.22 ($J_{Pt-H} = 63$ Hz) and δ 0.81 ($J_{Pt-H} = 60$ Hz), again consistent with inequivalent Pt(dppe)(Me) groups.

At high temperature (100 °C in DMSO-d_6), the four different dppe ^{31}P NMR signals coalesced into two, and one Pt−Me peak (δ 1.02 (d, $J = 7$, $J_{Pt-H} = 63$ Hz)) was observed by ^1H NMR spectroscopy. The resulting spectra were similar to those of the μ-PPh_2 complex **7** and consistent with the equivalence of the Pt(dppe)(Me) groups on the NMR time scale at high temperature, due to the conformational changes discussed above.

When a CD_2Cl_2 solution of **8** was cooled further (to −40 °C), NMR signals due to the two diastereomers **a** and **b** (7:1 ratio), which presumably result from compounds differing in the relative conformations of the Pt(dppe)(Me) groups, were

(12) Abraham, R. J. *The Analysis of High-Resolution NMR Spectra*; Elsevier: Amsterdam, 1971.

(13) Simulation with gNMR: Budzelaar, P. H. M. gNMR; Cherwell Scientific, 1992−1996.

(14) Pregosin, P. S.; Kunz, R. W. *^{31}P and ^{13}C NMR of Transition Metal Phosphine Complexes*; Springer-Verlag: New York, 1979.

Table 3. Selected ^{31}P NMR Data for Terminal and Bridging Phosphido Groups in the Complexes Pt(diphos)(Me)(PPh(R)) and [(Pt(diphos)(Me))$_2$(μ-PPh(R))][OTf]^a

complex	δ(PR$_2$)	J_{PP}(trans)	J_{Pt-P}(PR$_2$)	J_{Pt-P}(trans to PR$_2$)
Pt(dppe)(Me)(PPh$_2$) (**1**)	−7.8	144	1039	1932
[(Pt(dppe)(Me))$_2$(μ-PPh$_2$)][OTf] (**7**)	26.8	341	2313	2450
Pt(dppe)(Me)(PPh(*i*-Bu)) (**6**)	−29.9	134	946	1805
[(Pt(dppe)(Me))$_2$(μ-PPh(*i*-Bu))][OTf] (**8**)^b	0.8	337, 339	2243, 2319	2330, 2405
Pt(Me-Duphos)(Me)(PPh(*i*-Bu)) (**10**)^c	−57.3	129	999	1808
	−63.9	130	1011	1816
[(Pt(Me-Duphos)(Me))$_2$(μ-PPh(*i*-Bu))][OTf] (**11**)^d	5.5	334	2246	2292 (broad)^e
	−7.1	304	2307	

^{a} Chemical shift standard: external 85% H_3PO_4. Chemical shifts are given in ppm and coupling constants in Hz. Solvent: C_6D_6 for **1** and **6**, toluene-d_8 for **10**, CD_2Cl_2 for **7**, **8**, and **11**. Data for **1** and **6** are from ref 3a. ^{b} At -20 °C. ^{c} At -40 °C, two diastereomers. ^{d} At 21 °C, two diastereomers. ^{e} The expected two different Me-Duphos signals could not be resolved.

observed. The ^{31}P NMR data for these species were similar to those observed at higher temperature (Table 2).

Two diastereomers of **11** were also observed, but at room temperature. Again, we presume that these differ in the relative positions of the (Pt((*R*,*R*)-Me-Duphos)(Me)) moieties. The μ-phosphido signals, as in **8**, should show two different Pt−P couplings, but these peaks were simply broad triplets with only one J_{Pt-P} apparent. At 100 °C in CD_2Cl_4, the ^{31}P NMR spectrum of **11** showed broad peaks apparently due to a single species, perhaps because rotation about the Pt−P bonds was no longer slow on the NMR time scale. As expected, the four Me-Duphos P nuclei remained inequivalent at this temperature.[15] At −60 °C in CD_2Cl_2, four diastereomers were observed (see the Experimental Section); these formed two sets of isomers with similar μ-phosphido ^{31}P NMR chemical shifts (δ 2.9 and 2.6 vs δ −10.1 and −10.3).

From Terminal to Bridging Phosphido Ligands: Spectroscopic and Structural Consequences. The ^{31}P NMR data for the terminal and bridging phosphido complexes (Table 3) provided information on the changes in structure and bonding that result from the change in coordination mode. In addition to a substantial coordination chemical shift, both J_{PP} (trans) and J_{Pt-P} for the phosphido group increased significantly on quaternization. The small magnitudes of these couplings in terminal Pt−phosphido complexes have been ascribed to low s character in the Pt−P bonds, so that the lone pair in the pyramidal phosphido group has increased s character.[3a] Increased s character in the Pt−P bond as a result of the change in coordination number at P would rationalize the observed changes in these coupling constants; similar effects were seen on protonation of terminal phosphido complexes.[3a] Finally, the J_{Pt-P} value for the phosphine trans to the phosphido group also increased on coordination, consistent with a reduced trans influence for the μ-phosphido ligand in comparison to its terminal precursor.[16]

The Pt((*R*,*R*)-Me-Duphos) complexes **9**−**11** were characterized crystallographically (see Figures 2−4, Tables 4 and 5, and the Supporting Information), to obtain complementary data on the structural results of complexation of the metalloligand **10** to the Pt((*R*,*R*)-Me-Duphos)(Me) cation.[17] Although two diastereomers of **10** were observed by low-temperature ^{31}P NMR spectroscopy, the crystal studied contained only one, with an *R* configuration at the phosphido group. The unit cell of dinuclear **11** contained two independent molecules.

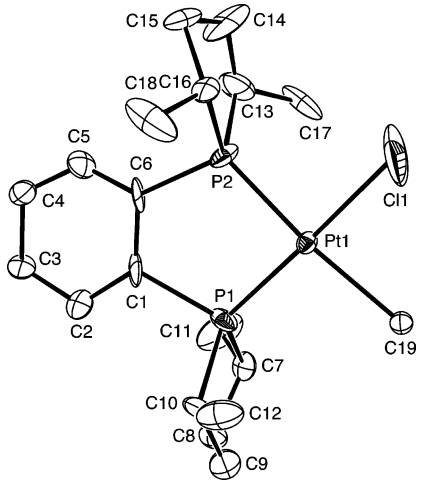

Figure 2. ORTEP diagram of Pt((*R*,*R*)-Me-Duphos)(Me)(Cl) (**9**).

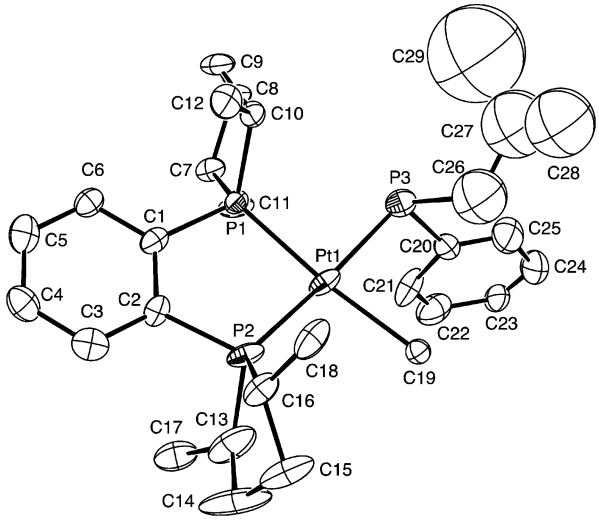

Figure 3. ORTEP diagram of Pt((*R*,*R*)-Me-Duphos)(Me)(PPh(*i*-Bu)) (**10**). The *i*-Bu group was disordered and refined with fixed geometry. The Pt−Me group (C19) was also disordered over two positions (48/52), only one of which is shown.

All three complexes adopted slightly distorted square planar geometries. As expected from the greater trans influence of Me in comparison to that of Cl, the Pt−P bond in **9** trans to the methyl group (2.223(5) Å) was longer than that trans to Cl (2.205(5) Å).[16] The Pt−Cl and Pt−P (trans to Cl) bond lengths in **9** (2.347(9) Å and 2.205(5) Å) were similar to those in Pt((*R*,*R*)-Me-Duphos)Cl$_2$·CH$_2$Cl$_2$ (2.3854(12) Å (average) and 2.2183(11) Å, respectively).[18] The average J_{Pt-P}(Duphos) values for the two diastereomers of **10** at −40 °C were 1768 Hz (trans to Me) and 1812 Hz (trans to PPh(*i*-Bu)). These data predict

(15) Similarly, the menthyl groups in tetrahedral Sn((−)-menthyl)$_2$(Ph)(I) were inequivalent: Dakternieks, D.; Dunn, K.; Henry, D. J.; Schiesser, C. H.; Tiekink, E. R. T. *Organometallics* **1999**, *18*, 3342−3347.

(16) Appleton, T. G.; Clark, H. C.; Manzer, L. E. *Coord. Chem. Rev.* **1973**, *10*, 335−422.

(17) For another example of structural comparisons before and after conversion of a terminal phosphido ligand to a bridging one, see ref 4c.

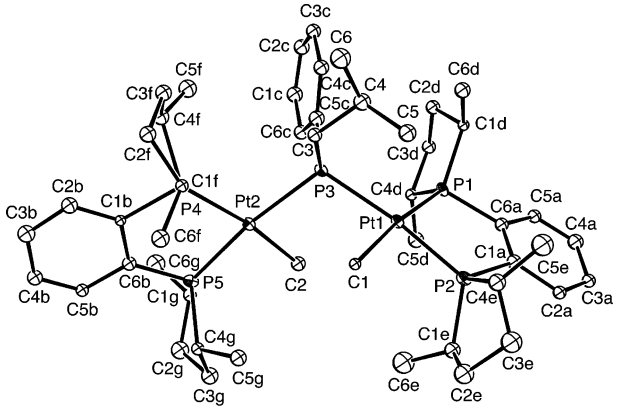

Figure 4. ORTEP diagram of [(Pt((*R*,*R*)-Me-Duphos)(Me))$_2$(μ-PPh(*i*-Bu))][OTf]·0.5THF (**11**), showing one of the two dinuclear cations. The triflate anion and the solvent are omitted for clarity.

Table 4. Crystallographic Data for Pt((*R*,*R*)-Me-Duphos)(Me)(Cl) (9), Pt((*R*,*R*)-Me-Duphos)(Me)(PPh(*i*-Bu)) (10), [(Pt(*R*,*R*)-Me-Duphos)(Me))$_2$(μ-PPh(*i*-Bu))][OTf]·0.5THF (11·0.5THF), and Pt(dppe)(Me)(P(O)Ph(*i*-Bu))·H$_2$O (12·H$_2$O)

	9	**10**	**11**·0.5THF	**12**·H$_2$O
formula	$C_{19}H_{31}ClP_2Pt$	$C_{29}H_{45}P_3Pt$	$C_{51}H_{80}F_3O_{3.50}P_5Pt_2S$	$C_{37}H_{43}O_2P_3Pt$
formula wt	551.92	681.65	1383.24	807.71
space group	$P4_3$	$P2_12_12_1$	$P1$	$P2_1/n$
a, Å	10.6441(7)	9.7296(6)	13.001(6)	9.446(2)
b, Å	10.6441(7)	15.4985(9)	13.676(7)	14.982(3)
c, Å	18.9672(19)	19.1019(12)	18.526(9)	25.135(6)
α, deg	90	90	82.144(7)	90
β, deg	90	90	71.255(7)	97.384(4)
γ, deg	90	90	61.738(6)	90
V, Å^3	2148.9(3)	2880.5(3)	2747(2)	3527.7(14)
Z	4	4	2	4
D(calcd), g/cm^3	1.706	1.572	1.672	1.521
μ(MoKα), mm^{-1}	6.801	5.054	5.321	4.144
temp, K	173(2)	100(2)	100(2)	213(2)
diffractometer	Bruker CCD			
R(*F*), %[a]	8.04	6.07	8.09	3.37
$R_w(F^2)$, %[a]	19.25	14.55	19.41	8.50

[a] Quantities minimized are as follows: $R_w(F^2) = \sum[w(F_o^2 - F_c^2)^2]/\sum[(wF_o^2)^2]^{1/2}$; $R = \sum\Delta/\sum(F_o)$ ($\Delta = |(F_o - F_c)|$; $w = 1/[\sigma^2(F_o^2) + (aP)^2 + bP]$; $P = [2F_c^2 + \mathrm{Max}(F_o,0)]/3$).

Table 5. Selected Bond Lengths (Å) and Angles (deg) for the Pt((*R*,*R*)-Me-Duphos)(Me)(X) Complexes 9, 10, and 11·0.5THF

	9 (X = Cl)	**10** (X = PPh(*i*-Bu))	**11**[b,c] (X = PPh(*i*-Bu))
Pt−P$_1$ (trans to Me)	2.223(5)	2.273(3)	2.301(5)
Pt−P$_2$ (trans to X)	2.205(5)	2.243(3)	2.255(6)
Pt−Me	2.264(13)	2.13(3)[a]	2.13(2)
Pt−X	2.347(9)	2.372(4)	2.394(6)
P$_1$−Pt−P$_2$	88.2(2)	86.44(12)	85.8(2)
P$_1$−Pt−Me	172.0(4)	171.0(9)[a]	171.8(6)
P$_1$−Pt−X	90.3(4)	90.45(12)	102.56(19)
P$_2$−Pt−Me	96.0(4)	91.6(7)[a]	86.9(6)
P$_2$−Pt−X	177.4(4)	175.71(13)	171.3(2)
C−Pt−X	85.7(5)	91.6(7)[a]	84.3(6)

[a] The Pt−Me group in **10** was disordered over two positions; average bond lengths and angles are reported. [b] [Pt((R,R)-Me-Duphos)(Me)]$^+$. There are two molecules in the unit cell; average bond lengths and angles are reported. [c] The average Pt−P$_3$−Pt angle was 109.5(2)°.

that the methyl group has a slightly larger trans influence, consistent with the Pt−P((*R*,*R*)-Me-Duphos) bond lengths observed in the solid state: 2.273(3) Å (trans to Me) and 2.243(3) Å (trans to PPh(*i*-Bu)).[19] The Pt−P(phosphido) bond in **10** (2.372(4) Å) was longer than the Pt−P((*R*,*R*)-Me-Duphos) bonds

Scheme 4[a]

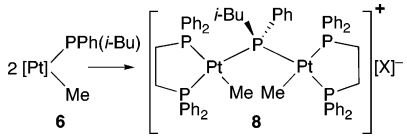

[a] [Pt] = Pt(dppe).

above, as observed in related Pt(diphos) phosphido complexes,[2d−h,3a] such as Pt((*R*,*R*)-Me-Duphos)(PPhIs)(H) (Is = 2,4,6-(*i*-Pr)$_3$C$_6$H$_2$; Pt−PR$_2$ = 2.335(5) Å, average Pt−Duphos = 2.262(5) Å).[2e]

When the metalloligand **10** was bound to Pt, the Pt−PR$_2$ bond lengthened slightly (from 2.372(4) to 2.394(6) Å). The sum of the angles at the phosphido P in **10** was 306.2(11)°; compare this pyramidal geometry to the ideal values for tetrahedral (328.5°) or trigonal-planar (360°) coordination or to 270° for unhybridized phosphorus (with the lone pair in an s orbital and P p orbitals used to make the P−R and Pt−P bonds). On coordination, this phosphorus became essentially tetrahedral. For the two independent molecules of **11**, the angles about P$_3$ ranged from 120.4(7) to 100.8(10)°; the average was 109.5°. This change in geometry at phosphorus is consistent with the increased steric demands of the lone pair in the terminal phosphido complex **10**[20] and with increased s character in the Pt−P bonds (P sp^3 hybridization), as discussed above in the context of the ^{31}P NMR data.

The NMR results also predicted that the terminal phosphido ligand in **10** would have a greater trans influence than the bridging ligand in **11**.[16] However, the appropriate Pt−P(Duphos) bond lengths in these compounds (2.243(3) and 2.255(6) Å) were not significantly different; therefore, this effect could not be confirmed from the crystallographic data. Finally, the relative conformations of the Pt(diphos)(Me) groups in the solid state are relevant to the fluxional processes observed in solution, where these groups could become equivalent when coplanar (conformation **B** above). The average dihedral angle between the two Pt square planes in **11** was 76.4°, comparable to that observed in **5** (71.1(2)°); both μ-phosphido complexes displayed restricted rotation about the Pt−μ-PR$_2$ bonds.[3c]

From Terminal to Bridging Coordination: An Alternative Route. We also observed formation of **8** via decomposition of **6** (Scheme 4). Yellow solutions of **6** slowly deposited white solid **8** at room temperature; the reaction was faster on heating. It was difficult to induce complete conversion to **8**, but filtration enabled separation from **6**. Solid **8** formed by this route was soluble in polar solvents and could be recrystallized from CH$_2$Cl$_2$/ether to give a white powder. NMR and mass spectroscopy confirmed that cation **8** formed, but how did this happen, and what was the anion X$^-$?

We considered several potential pathways for decomposition of **6** to give **8** (Scheme 5). Most simply, attack of the phosphido ligand at the Pt center in another molecule of **6** could displace the anion [PPh(*i*-Bu)]$^-$ and give cation **8**. However, neither this known anion[21] nor the secondary phosphine PHPh(*i*-Bu), which would form from it on protonation by adventitious acid, were observed during the decomposition of **6**. Alternatively, oxidation of **6** by traces of oxygen might produce a better leaving group

(18) Wicht, D. K.; Zhuravel, M. A.; Gregush, R. V.; Glueck, D. S.; Guzei, I. A.; Liable-Sands, L. M.; Rheingold, A. L. *Organometallics* **1998**, *17*, 1412−1419.
(19) Appleton, T. G.; Bennett, M. A. *Inorg. Chem.* **1978**, *17*, 738−747.
(20) Bonnet, G.; Kubicki, M. M.; Moise, C.; Lazzaroni, R.; Salvadori, P.; Vitulli, G. *Organometallics* **1992**, *11*, 964−967.

Scheme 5. Possible Routes for Formation of Cation 8 from 6[a]

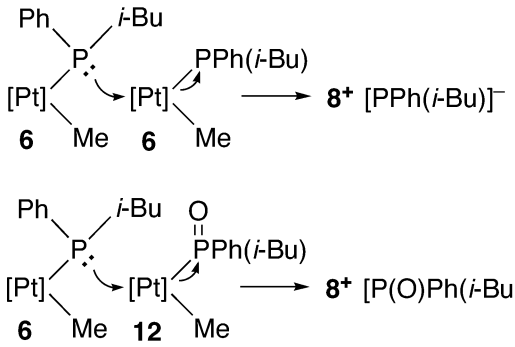

[a] [Pt] = Pt(dppe).

Scheme 6[a]

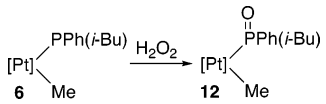

[a] [Pt] = Pt(dppe).

in the P(O)Ph(*i*-Bu) ligand, which could again be displaced by the Pt−PPh(*i*-Bu) group.

We tested the latter hypothesis by preparing the phosphido oxide complex Pt(dppe)(Me)(P(O)Ph(*i*-Bu)) (**12**) by oxidation of **6** with H_2O_2 (Scheme 6; it also formed on exposure of **6** to air).[22] The ^{31}P NMR chemical shifts of the dppe and phosphido oxide P atoms in **12** were similar, but they could be assigned on the basis of their Pt−P coupling constants. On oxidation of *trans*-Pt(PCy_2H)$_2$(PCy_2)(Cl) to *trans*-Pt(PCy_2H)$_2$(P(O)Cy_2)(Cl), J_{Pt-P} for the phosphido ligand changed from 931 to 3078 Hz.[2c,22a] Similarly, J_{Pt-P} for the P(O)Ph(*i*-Bu) ligand in **12** increased to 3006 Hz from 946 Hz in **6**.[3a] J_{Pt-P} for the dppe P trans to this ligand decreased from 1805 to 1714 Hz, consistent with a greater trans influence for the phosphido oxide than for the phosphido ligand.[3a,23] The change in trans J_{PP} on oxidation of **6** to **12** (from 134 to 411 Hz) is consistent with the trend in J_{Pt-P} and increased s character in the Pt−P bond.[3a]

The crystal structure of **12·H$_2$O** (see Figure 5 and Table 4) showed distorted-tetrahedral geometry at P and the presence of a water molecule hydrogen-bonded to the P═O group.[24] The O···O distance of 2.667 Å is similar to that found in related hydrogen-bonded adducts of triphenylphosphine oxide.[25]

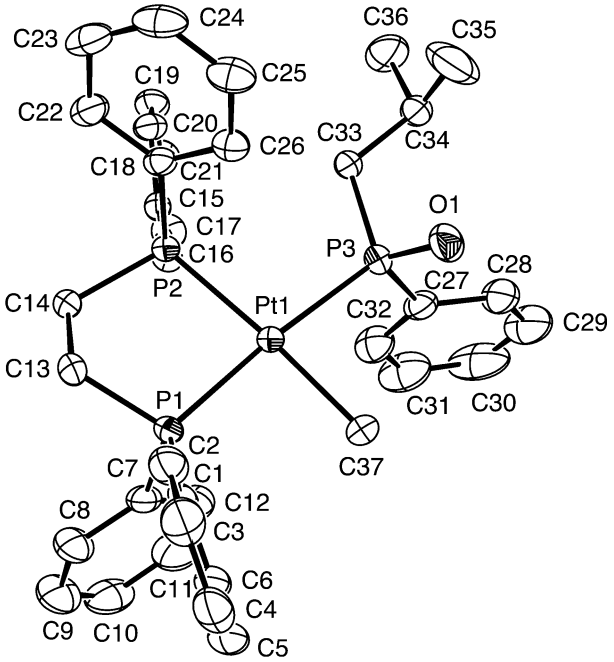

Figure 5. ORTEP diagram of Pt(dppe)(Me)(PPh(*i*-Bu)O)·H_2O (**12**·H_2O). The water molecule and the hydrogen atoms are not shown (a partial ORTEP diagram which illustrates the hydrogen bonding is given in the Supporting Information).

When **6** and oxide **12** were combined, cation **8** formed slowly, as it did in the absence of **12**. Thus, inadvertent oxidation to yield **6-O** does not appear to promote cation formation as proposed in Scheme 5.

To further probe the formation of **8** from **6**, we studied the decomposition of **6** under a variety of conditions, including deliberate addition of air, water, and the secondary phosphine PHPh(*i*-Bu). Cation **8** was reproducibly formed in each case, along with a varied mixture of unidentified phosphorus products, observed by ^{31}P NMR spectroscopy (see the Experimental Section). As mentioned above, these did not include the anion [PPh(*i*-Bu)]$^-$ or PHPh(*i*-Bu). Other potential products, including the secondary phosphine oxide PH(O)Ph(*i*-Bu), its anion [P(O)Ph(*i*-Bu)]$^-$, commercially available P(O)Ph(*i*-Bu)(OH), and its anion [PO_2Ph(*i*-Bu)]$^-$, were generated for comparison to reaction mixtures (see the Experimental Section), but the fate of the PPh(*i*-Bu) group could not be determined. Attempts to identify the anion (or anions) in cation **8** by elemental analyses and mass spectroscopy were also unsuccessful.

Conclusions

The terminal phosphido complexes Pt(diphos)(Me)(PPh(R)) (**1**, **6**, and **10**) acted as ligands to the [Pt(diphos)(Me)]$^+$ fragment, yielding the dinuclear μ-phosphido complexes [(Pt(diphos)(Me))$_2$(μ-PPh(R))]$^+$ (**7**, **8**, and **11**). Fluxional behavior in the unsymmetrically bridged cations **8** and **11** was consistent with restricted rotation about the Pt−PPh(*i*-Bu) bonds; it resulted in two diastereomers for **8** and four for **11** at low temperature. Comparison of the ^{31}P NMR data before and after complexation and the X-ray crystal structures of **10** and **11** were consistent with changes in the geometry at phosphorus (from distorted pyramidal, with a stereochemically active lone pair, to tetrahe-

(21) Treatment of PHPh(*i*-Bu) with *s*-BuLi in petroleum ether gave a white precipitate, presumably LiPPh(*i*-Bu), which was redissolved in THF for ^{31}P NMR characterization. The observed chemical shift was surprisingly close to that of the phosphine, but direct reaction of PHPh(*i*-Bu) and *s*-BuLi in THF gave the same results. This material was not soluble in toluene, preventing direct comparison with the results from decomposition of **6**. The observed chemical shifts are consistent with an earlier report: Grim, S. O.; Molenda, R. P. *Phosphorus Relat. Group V Elem.* **1974**, *4*, 189−193.

(22) For oxidation of terminal phosphido complexes, see: (a) Mastrorilli, P.; Latronico, M.; Nobile, C. F.; Suranna, G. P.; Fanizzi, F. P.; Englert, U.; Ciccarella, G. *Dalton Trans.* **2004**, 1117−1119. (b) Giner Planas, J.; Gladysz, J. A. *Inorg. Chem.* **2002**, *41*, 6947−6949. (c) Buhro, W. E.; Zwick, B. D.; Georgiou, S.; Hutchinson, J. P.; Gladysz, J. A. *J. Am. Chem. Soc.* **1988**, *110*, 2427−2439. (d) Buhro, W. E.; Georgiou, S.; Hutchinson, J. P.; Gladysz, J. A. *J. Am. Chem. Soc.* **1985**, *107*, 3346−3348. (e) Ebsworth, E. A. V.; Gould, R. O.; McManus, N. T.; Rankin, D. W. H.; Walkinshaw, M. D.; Whitelock, J. D. *J. Organomet. Chem.* **1983**, *249*, 227−242.

(23) We have observed the same trans influence ordering in related Pt(Me-Duphos) phosphido complexes and their oxidized derivatives: Scriban, C.; Glueck, D. S.; DiPasquale, A. G.; Dougherty, W.; Rheingold, A. L. Manuscript in preparation.

(24) Edmundson, R. S. Chemical Properties and Reactions of Phosphine Chalcogenides. In *The Chemistry of Organophosphorus Compounds*; Hartley, F. R., Ed.; Wiley: Chichester, U.K., 1992; Vol. 2, pp 287−407.

(25) (a) Chandrasekhar, S.; Kulkarni, G.; Muktha, B.; Row, T. N. G. *Tetrahedron: Asymmetry* **2003**, *14*, 3769−3772. (b) Steiner, T. *Acta Crystallogr., Sect. C: Cryst. Struct. Commun.* **2000**, *C56*, 1033−1034. (c) Gramstad, T.; Husebye, S.; Maartmann-Moe, K. *Acta Chem. Scand.* **1986**, *B40*, 26−30.

dral) on conversion of the terminal phosphido ligand to a bridging group.

Experimental Section

Unless otherwise noted, all reactions and manipulations were performed in dry glassware under a nitrogen atmosphere at 20 °C in a drybox or using standard Schlenk techniques. Petroleum ether (bp 38−53 °C), ether, THF, toluene, and CH_2Cl_2 were dried using columns of activated alumina.[26] Deuterated solvents used for NMR spectroscopy were dried over molecular sieves and degassed. NMR spectra were recorded using Varian 300 and 500 MHz spectrometers. ^{1}H and ^{13}C NMR chemical shifts are reported vs Me_4Si and were determined by reference to the residual ^{1}H and ^{13}C solvent peaks. ^{31}P NMR chemical shifts are reported vs H_3PO_4 (85%) used as an external reference. Coupling constants are reported in Hz, as absolute values unless noted otherwise. Unless indicated, peaks in NMR spectra are singlets. IR spectra were obtained on KBr pellets and are reported in cm^{-1}. Elemental analyses were provided by Schwarzkopf Microanalytical Laboratory. Mass spectra were recorded at the University of Illinois Urbana-Champaign. Unless otherwise noted, reagents were obtained from commercial suppliers. The following compounds were made by the literature procedures: Pt(COD)(Me)Cl,[7] Pt(dppe)(Me)(Cl).[6] The phosphido complexes Pt(dppe)(Me)(PPh(R)) (R = Ph, *i*-Bu) were prepared as previously reported[3a] or by the new method described below.

Pt(dppe)(Me)(PPh(*i*-Bu)) (6). We previously reported the synthesis of this complex by treatment of Pt(dppe)(Me)(OMe) with PHPh(*i*-Bu).[3a] Since the Pt−methoxide complex was made from Pt(dppe)(Me)(Cl), the new procedure is more convenient. PHPh(*i*-Bu) (41.6 mg, 0.25 mmol) was added with a microsyringe to a stirred slurry of Pt(dppe)(Me)(Cl) (161 mg, 0.25 mmol) in toluene (20 mL). $NaOSiMe_3$ (28.1 mg, 0.25 mmol) in toluene (10 mL) was added to the reaction mixture, which turned yellow; a white precipitate formed. The slurry was filtered through Celite, and the yellow filtrate was concentrated under vacuum. Petroleum ether was added to the yellow residue, yielding a yellow precipitate, which was washed further with petroleum ether. Drying the precipitate yielded 155 mg (80%) of yellow powder. Pt(dppe)(Me)(PPh_2) was prepared similarly (82% yield).

[(Pt(dppe)(Me))$_2$(μ-PPh$_2$)][OTf] (7). A solution of AgOTf (51.4 mg, 0.2 mmol) in 2 mL of THF was added to a stirred slurry of Pt(dppe)(Me)(Cl) (128.8 mg, 0.2 mmol) in 10 mL of THF. A white precipitate formed immediately. The slurry was filtered through Celite, and the filtrate was added to a bright yellow solution of Pt(dppe)(Me)(PPh_2) (**1**; 158.8 mg, 0.2 mmol) in 10 mL of THF. The white precipitate that formed in about 5 min was washed with THF (three 5 mL portions) and dried under vacuum, yielding 195 mg (63%) of white powder. The white powder was dissolved in the minimum amount of CH_2Cl_2 and cooled to −25 °C overnight, yielding white crystals.

Anal. Calcd for $C_{67}H_{64}F_3O_3P_5Pt_2S$: C, 51.87; H, 4.16. Found: C, 52.07; H, 4.32. ^{31}P{^{1}H} NMR (CD_2Cl_2; see Table 2): δ 52.3 (broad dd, J = 341, 16, J_{Pt-P} = 2450), 49.2 (broad d, J = 16, J_{Pt-P} = 1895), 26.8 (apparent tt with fine structure on the central peak, J = 341, 16, J_{Pt-P} = 2313). ^{1}H NMR (CD_2Cl_2): δ 7.67−7.49 (broad m, 12H, Ar), 7.49−7.42 (broad m, 8H, Ar), 7.35 (td, J = 7, 2, 4H, Ar), 7.22−7.19 (m, 8H, Ar), 7.18−7.14 (m, 8H, Ar), 7.00−6.97 (m, 2H, Ar), 6.88−6.84 (m, 4H, Ar), 6.68−6.63 (m, 4H, Ar), 2.12−1.90 (m, 8H), 0.91−0.86 (m, 6H, J_{Pt-H} = 61, Pt−Me).

[(Pt(dppe)(Me))$_2$(μ-PPh(*i*-Bu))][OTf] (8). A solution of AgOTf (51.4 mg, 0.2 mmol) in 2 mL of THF was added to a stirred slurry of Pt(dppe)(Me)(Cl) (128.8 mg, 0.2 mmol) in 5 mL of THF. A white precipitate formed immediately. The slurry was filtered through Celite, and the filtrate was added to a bright yellow solution of Pt(dppe)(Me)(PPh(*i*-Bu)) (**6**; 154.8 mg, 0.2 mmol) in 5 mL of THF. The reaction mixture turned off-white. The solvent was removed under vacuum, and petroleum ether was added to the viscous residue, yielding a light yellow precipitate, which was dried under vacuum to yield 200 mg (65%) of light yellow powder. We were unable to remove trace impurities by recrystallization from CH_2Cl_2/ether; thus, analytically pure material was not obtained.

Anal. Calcd for $C_{65}H_{68}F_3O_3P_5Pt_2S$: C, 50.98; H, 4.48. Found: C, 49.61; H, 4.72. HRMS (*m*/*z*): calcd, 1381.3305; found, 1381.3474. See Table 2 and the accompanying discussion for more information on the temperature-dependent ^{31}P NMR spectra. ^{31}P{^{1}H} NMR (CD_2Cl_2): δ 52.8 (broad d, J = 329, J_{Pt-P} = 2338), 50.5 (broad d, J = 352, J_{Pt-P} = 2408), 48.5 (broad, J_{Pt-P} = 1906), 47.6 (broad, J_{Pt-P} = 1800), 1.0 (apparent tt, "J" = 339, 15, apparent J_{Pt-P} = 2289). ^{31}P{^{1}H} NMR (CD_2Cl_2, −20 °C): δ 53.2 (dd, J = 337, 6, J_{Pt-P} = 2330), 50.4 (dd, J = 339, 4, J_{Pt-P} = 2405), 48.6 (d, J = 15, J_{Pt-P} = 1886), 47.2 (d, J = 15, J_{Pt-P} = 1863), 0.8 (overlapping ddt, J = 339, 337, 15, J_{Pt-P} = 2243, 2319). ^{31}P{^{1}H} NMR (CD_2Cl_2, −40 °C): δ 53.9 (broad d, J = 334, J_{Pt-P} = 2331, **b**), 53.5 (d, J = 334, J_{Pt-P} = 2331, **a**), 50.7 (broad d, J = 340, J_{Pt-P} = 2405, **b**), 50.4 (d, J = 340, J_{Pt-P} = 2405, **a**), 49.1 (broad, J_{Pt-P} = 1903, **b**), 48.7 (d, J = 15, J_{Pt-P} = 1889, **a**), 47.4 (broad, J_{Pt-P} = 1883, **b**), 47.0 (d, J = 15, J_{Pt-P} = 1864, **a**), 1.2 (broad t, "J" = 338, **b**), 0.9 (tt, J = 340, 334, 15, J_{Pt-P} = 2319, 2231, **a**). ^{31}P{^{1}H} NMR (DMSO-d_6, 100 °C): δ 51.7 (d, J = 338, J_{Pt-P} = 2382), 48.3 (apparent d, J = 15, J_{Pt-P} = 1871), 2.3 (apparent t, J = 338, apparent J_{Pt-P} = 2280). ^{1}H NMR (DMSO-d_6, 21 °C; the signals were broad, so it was not possible to integrate them all reliably; peaks are assigned where possible): δ 7.80−7.62 (m, 4H, Ar), 7.62−7.50 (m, 14H, Ar), 7.50−7.40 (broad m, 10H, Ar), 7.40−7.12 (m, 7H, Ar), 7.12−7.06 (m, 2H, Ar), 7.06−6.90 (broad, 2H, Ar), 6.76−6.70 (m, 2H, Ar), 6.70−6.63 (m, 2H, Ar), 6.56−6.36 (broad, 2H, Ar), 2.50 (m, 1H, CH), 2.45−2.30 (m, 2H, CH_2), 2.30−1.60 (broad m, CH_2), 1.30−1.00 (broad m, 3H, Pt−CH_3), 0.90−0.55 (broad m, 3H, Pt−CH_3), 0.55−0.35 (broad m, CH_3), 0.35−0.10 (broad m, CH_3). ^{1}H NMR (DMSO-d_6, 100 °C): δ 7.67−7.50 (m, 16H, Ar), 7.49−7.43 (m, 6H, Ar), 7.43−7.38 (m, 2H, Ar), 7.38−7.32 (m, 4H, Ar), 7.32−7.25 (m, 8H, Ar), 7.25−7.10 (broad m, 4H, Ar), 7.09−7.03 (m, 1H, Ar), 6.88−6.81 (m, 2H, Ar), 6.76−6.71 (m, 2H, Ar), 2.51−2.50 (m, 1H, CH), 2.45−2.25 (m, 4H, CH_2), 2.20−2.00 (m, 4H, CH_2), 1.70−1.60 (broad, 2H, CH_2), 1.02 (d, J = 7, J_{Pt-H} = 63, 6H, Pt-Me), 0.50 (d, J = 6, 6H, Me).

Pt((*R*,*R*)-Me-Duphos)(Me)(Cl) (9). A solution of (*R*,*R*)-Me-Duphos (173 mg, 0.565 mmol) in CH_2Cl_2 (2 mL) was added dropwise to a solution of Pt(COD)(Me)(Cl) (200 mg, 0.565 mmol) in CH_2Cl_2 (3 mL) to give a pale yellow solution. In the air, the solvent was removed under reduced pressure and the remaining crystals were washed with Et_2O (3 × 2 mL) and recrystallized from CH_2Cl_2/Et_2O at −25 °C to yield 247 mg (79%) of white crystals, suitable for single-crystal X-ray diffraction.

Anal. Calcd for $C_{19}H_{31}ClP_2Pt$: C, 41.35; H, 5.66. Found: C, 41.31; H, 5.74. ^{31}P{^{1}H} NMR ($CDCl_3$): δ 72.3 (d, J = 4, J_{Pt-P} = 1722), 61.4 (d, J = 4, J_{Pt-P} = 4065). ^{1}H NMR ($CDCl_3$): δ 7.69−7.63 (m, 2H, Ar), 7.57−7.55 (m, 2H, Ar), 3.24−3.18 (m, 1H), 3.06−2.96 (m, 1H), 2.82−2.69 (m, 2H), 2.40−2.25 (m, 4H), 2.02−1.94 (m, 1H), 1.89−1.63 (m, 3H), 1.45−1.40 (dd, J = 18, 7, 3H, Me), 1.29−1.24 (dd, J = 18, 7, 3H, Me), 0.90−0.86 (dd, J = 15, 7, 3H, Me), 0.86−0.82 (dd, J = 15, 7, 3H, Me), 0.71−0.60 (dd, J = 7, 2, J_{Pt-H} = 53, 3H, Me). ^{13}C{^{1}H} NMR ($CDCl_3$): δ 144.2 (dd, J = 38, 49, quat), 142.6 (dd, J = 25, 36, quat), 133.1 (d, J = 13, Ar), 132.1 (dd, J = 4, 15, Ar), 131.3−131.1 (m, Ar), 40.8 (d, J = 26), 40.1 (d, J = 39), 37.3−36.7 (m), 35.6 (d, J = 26), 17.2 (3-line pattern, Me), 14.4 (d, J = 2, Me), 14.1 (Me), 6.5 (dd, J = 6, 97, Pt−Me).

Pt((*R*,*R*)-Me-Duphos)(Me)(PPh(*i*-Bu)) (10). PHPh(*i*-Bu) (33.2 mg, 0.2 mmol) was added with a microsyringe to a stirred slurry of Pt((*R*,*R*)-Me-Duphos)(Me)(Cl) (110.4 mg, 0.2 mmol) in toluene

(26) Pangborn, A. B.; Giardello, M. A.; Grubbs, R. H.; Rosen, R. K.; Timmers, F. J. *Organometallics* **1996**, *15*, 1518−1520.

(20 mL). $NaOSiMe_3$ (22.4 mg, 0.2 mmol) in toluene (10 mL) was added to the reaction mixture, which turned yellow. After it was stirred for 12 h, the slurry was filtered through Celite, and the yellow filtrate was concentrated under vacuum. Petroleum ether was added to the yellow residue, yielding a yellow precipitate, which was washed further with petroleum ether. Drying the precipitate yielded 122 mg (90%) of yellow powder. The following NMR spectra are reported for the mixture of two diastereomers **a** and **b** (ratio 1.2:1), unless otherwise indicated. Recrystallization from petroleum ether at −25 °C gave X-ray-quality crystals.

Anal. Calcd for $C_{29}H_{45}P_3Pt$: C, 51.10; H, 6.65. Found: C, 50.70; H, 7.07. $^{31}P\{^1H\}$ NMR (21 °C, C_6D_6): δ 67.6 (broad d, $J = 116$, $J_{Pt-P} = 1779$, **a**), 62.7 (broad, $J_{Pt-P} = 1776$, **a**), −61.3 (broad d, $J = 120$, $J_{Pt-P} = 1026$, **a**), 66.3 (d, broad, $J = 116$, Pt satellites not resolved, **b**), 62.6 (broad, $J_{Pt-P} = 1743$, **b**), −56.7 (broad d, $J = 108$, $J_{Pt-P} = 970$, **b**). $^{31}P\{^1H\}$ NMR (−40 °C, toluene-d_8; diastereomer **a**): δ 69.6 (dd, $J = 131$, 8, $J_{Pt-P} = 1816$), 64.2 (dd, $J = 21$, 9, $J_{Pt-P} = 1768$), −63.9 (dd, $J = 130$, 18, $J_{Pt-P} = 1011$). $^{31}P\{^1H\}$ NMR (−40 °C, toluene-d_8; diastereomer **b**): δ 67.8 (dd, $J = 128$, 8, $J_{Pt-P} = 1808$), 64.2 (dd, $J = 21$, 9, $J_{Pt-P} = 1768$), −57.3 (dd, $J = 129$, 23, $J_{Pt-P} = 999$). The chemical shift for the cis phosphorus, as well as J_{Pt-P}, was the same for both diastereomers. ^1H NMR (C_6D_6): δ 7.93 (broad, 2H, Ar), 7.33−7.30 (m, 1H, Ar), 7.28−7.25 (m, 2H, Ar), 7.21−7.18 (m, 1H, Ar), 7.06−6.99 (m, 3H, Ar), 3.65−3.62 (m, 1H, CH), 2.80−2.66 (broad, 1H), 2.58−2.47 (m, 2H), 2.40−2.31 (m, 2H), 2.23−2.16 (m, 1H), 2.08−2.00 (m, 2H), 1.90−1.70 (m, 2H), 1.56−1.46 (m, 1H), 1.51 (dd, $J = 18$, 7, 3H, Me), 1.45−1.35 (m, 1H), 1.33 (d, $J = 7$, 6H, Me), 1.31−1.24 (m, 2H), 1.21 (td, $J = 7$, 3, 3H, Pt−Me), 1.15 (dd, $J = 18$, 7, 3H, Me), 0.76 (dd, $J = 14$, 7, 3H, Me), 0.64 (dd, $J = 14$, 7, 3H, Me). $^{13}C\{^1H\}$ NMR (C_6D_6): δ 147.4 (m, quat), 145.8−145.5 (m, quat), 133.2 (dd, $J = 50$, 14, Ar), 130.2 (dm, $J = 42$, Ar), 128.3 (Ar), 127.0 (d, $J = 3$, Ar), 123.9 (m, Ar), 41.5 (d, $J = 27$), 40.8 (d, $J = 26$), 37.7−37.4 (m), 36.9 (m), 35.5−34.9 (m), 34.4−33.5 (m), 29.5 (broad), 25.5 (d, $J = 7$), 25.2 (broad), 22.7, 17.5−17.0 (m), 14.2 (d, $J = 8$), 13.9.

[Pt((*R*,*R*)-Me-Duphos)(Me))$_2$(μ-PPh(*i*-Bu))][OTf] (11). A solution of AgOTf (19.8 mg, 0.08 mmol) in 2 mL of THF was added to a solution of Pt((*R*,*R*)-Me-Duphos)(Me)(Cl) (42.5 mg, 0.08 mmol) in 5 mL of THF. A white precipitate formed immediately. The slurry was filtered through Celite, and the filtrate was added to a yellow solution of Pt((*R*,*R*)-Me-Duphos)(Me)(PPh(*i*-Bu)) (52.5 mg, 0.08 mmol) in 5 mL of THF, yielding a colorless solution. The solution was concentrated under vacuum, and petroleum ether was added to the white residue, yielding a white precipitate. The precipitate was washed with petroleum ether (three 3 mL portions) and dried under vacuum, yielding 90 mg (87%) of a white powder, which was recrystallized from THF and petroleum ether to give crystals of a THF solvate suitable for X-ray crystallography. A sample for elemental analysis, recrystallized from THF/petroleum ether, also contained THF, as quantified by integration of the ^1H NMR spectrum in CD_2Cl_2.

At room temperature in CD_2Cl_2, the two diastereomers **a** and **b** were observed in a 2.5:1 ratio. At low temperature, the four diastereomers $\mathbf{a}_1$, $\mathbf{a}_2$, $\mathbf{b}_1$, and $\mathbf{b}_2$ (1.7:2.3:1:1.4 ratio) were observed. The following NMR spectra are reported for the mixture, with assignments given where possible.

Anal. Calcd for $C_{49}H_{76}F_3O_3P_5Pt_2S\cdot 0.2C_4H_8O$: C, 43.93; H, 5.74. Found: C, 44.25; H, 5.69. $^{31}P\{^1H\}$ NMR (CD_2Cl_2): δ 69.3 (broad, $J_{Pt-P} = 1840$), 67.5 (broad d, $J = 334$, $J_{Pt-P} = 2292$), 65.2 (broad, $J_{Pt-P} = 1750$), 5.5 (broad t-like pattern, $J = 336$, $J_{Pt-P} = 2246$, **a**), −7.1 (broad t-like pattern, $J = 304$, $J_{Pt-P} = 2307$, **b**). ^1H NMR (CD_2Cl_2): δ 7.94 (broad, 2H, Ar), 7.76−7.71 (m, 2H, Ar), 7.67−7.62 (m, 2H, Ar), 7.60−7.54 (m, 4H, Ar), 7.30−7.26 (m, 2H, Ar), 7.18−7.14 (m, 1H, Ar), 3.20−1.50 (m, 27H, CH + CH_2), 1.44−0.98 (m, 21H, Me), 0.92−0.81 (m, 12H, Me), 0.50−0.18 (broad, 3H, Me). $^{31}P\{^1H\}$ NMR (CD_2Cl_2, −60 °C, selected signals (not all the Me-Duphos peaks could be resolved/assigned)): δ 68.7 ($J_{Pt-P} = 1797$), 68.4 ($J_{Pt-P} = 1803$), 67.2 (d, $J = 339$), 66.9 (d, $J = 339$), 66.6 (d, $J = 328$), 66.0 (d, $J = 331$), 65.2 ($J_{Pt-P} = 1849$), 64.9 ($J_{Pt-P} = 1860$), 64.2 ($J_{Pt-P} = 1864$), 63.9 ($J_{Pt-P} = 1858$), 2.9 (broad t, $J = 334$, $J_{Pt-P} = 2300$, $\mathbf{a}_1$), 2.6 (tt-like pattern, $J = 331$, 14, $J_{Pt-P} = 2300$, $\mathbf{a}_2$), −10.1 (broad t, $J = 335$, $J_{Pt-P} = 2240$, $\mathbf{b}_1$), −10.3 (tm, $J = 335$, $J_{Pt-P} = 2240$, $\mathbf{b}_2$). $^{31}P\{^1H\}$ NMR (CD_2Cl_4, 100 °C): δ 66.6 (broad, $J_{Pt-P} = 1834$), 65.9 (broad d, $J = 340$, $J_{Pt-P} = 2325$), 65.8 (broad d, $J = 335$, $J_{Pt-P} = 2330$), 65.6 (broad, $J_{Pt-P} = 1801$), −2.1 (very broad).

Decomposition of Pt(dppe)(Me)(PPh(*i*-Bu)) (6). A bright yellow solution of Pt(dppe)(Me)(PPh(*i*-Bu)) (**6**; 143 mg, 0.185 mmol) in toluene (15 mL) was heated in a sealed ampule at 50 °C for 3 days, during which time a white precipitate formed and the solution became pale yellow. The first crop was collected on a fine frit, washed with petroleum ether, and dried to give 21 mg of an off-white solid. The yellow mother liquor was heated for an additional week to give a second crop (81 mg). The combined crops were recrystallized from CH_2Cl_2/ether at −25 °C to give 70 mg of white solid (54%; calculated for [(Pt(dppe)(Me))$_2$(μ-PPh(*i*-Bu))][OH], since the nature of the anion is not known).

Anal. Calcd for $C_{64}H_{68}P_5Pt_2OH$ (**8-OH**): C, 54.94; H, 4.97. Anal. Calcd for $C_{64}H_{68}P_5Pt_2Cl$ (**8-Cl**): C, 54.22; H, 4.83. Found: C, 53.61; H, 5.36. $^{31}P\{^1H\}$ NMR: see Table 2 and data for the triflate salt above. $^1H\{^{31}P\}$ NMR (CD_2Cl_2, −60 °C; relative integrals are not reported, signals are assigned where possible): δ 7.87−7.84 (m, Ar), 7.81−7.78 (m, Ar), 7.65−7.32 (m, Ar), 7.18−7.11 (m, Ar), 7.04−7.00 (m, Ar), 6.93−6.86 (broad m, Ar), 6.67−6.62 (m, Ar), 6.51−6.48 (broad, Ar), 6.23−6.21 (m, Ar), 2.68−2.63 (m), 2.27−2.04 (m), 1.84−1.58 (m), 1.22 ($J_{Pt-H} = 63$, Pt−Me), 0.81 ($J_{Pt-H} = 60$, Pt−Me), 0.76 (broad), 0.15 (broad). Low-resolution FAB MS (Magic Bullet; *m*/*z*): 1535.5, 1415.3, 1381.3 (M^+), 1365.2, 1289.2, 1109.2, 791.1, 773.1, 758.1, 717.1, 702.1, 678.9, 634.9, 592.0, 558.9, 527.8, 484.9, 408.9, 301.9, 183.0. IR: 3044, 2922, 1622, 1483, 1433, 1411, 1311, 1183, 1100, 1000, 878, 822, 744, 700, 533, 489.

The decomposition of **6** was repeated several times in analogous experiments, with monitoring by ^{31}P NMR spectroscopy, in attempts to identify the anion of **8** and the fate of the PPh(*i*-Bu) group (see Scheme 5 and related discussion above). For details of these experiments, see the Supporting Information.

Pt(dppe)(Me)(P(O)Ph(*i*-Bu)) (12). Pt(dppe)(Me)(PPh(*i*-Bu)) (101 mg, 0.13 mmol) was dissolved in 5 mL of toluene to yield a yellow solution, which was transferred to an NMR tube fitted with a rubber septum. H_2O_2 (30% in H_2O, 30 μL, 0.26 mmol) was added with a microliter syringe. The reaction mixture turned into a white suspension, and gas evolved. ^{31}P NMR spectroscopy indicated the formation of Pt(dppe)(Me)(P(O)Ph(*i*-Bu)) (**12**). The solvent was removed under vacuum, and the white residue was washed with petroleum ether (three 3 mL portions). Drying the precipitate yielded 95 mg (93%) of white powder. Recrystallization from CD_2Cl_2 and petroleum ether at 5 °C gave crystals of a monohydrate, as observed by X-ray crystallography and elemental analysis.

Anal. Calcd for $C_{37}H_{41}OP_3Pt\cdot H_2O$: C, 55.02; H, 5.37. Found: C, 54.72; H, 5.48. $^{31}P\{^1H\}$ NMR (C_6D_6): δ 58.7 (dd, $J = 411$, 23, $J_{Pt-P} = 3006$), 48.6 (d, $J = 23$, $J_{Pt-P} = 1897$), 46.4 (d, $J = 411$, $J_{Pt-P} = 1714$). ^1H NMR (CD_2Cl_2): δ 7.90−7.86 (m, 2H, Ar), 7.65−7.58 (m, 6H, Ar), 7.53−7.39 (m, 12H, Ar), 7.32 (td, $J = 8$, 2, 2H, Ar), 7.20−7.19 (m, 3H, Ar), 2.36−1.96 (m, 6H), 1.58−1.54 (m, 1H), 0.98 (d, $J = 7$, 3H, CH_3, *i*-Bu), 0.75 (d, $J = 7$, 3H, CH_3, *i*-Bu), 0.57 (m, $J_{Pt-H} = 66$, 3H, Pt−CH_3). $^{13}C\{^1H\}$ NMR (CD_2Cl_2): δ 134.3 (d, $J = 11$, Ar), 134.0 (d, $J = 12$, Ar), 133.8 (d, $J = 2$, Ar), 133.7 (d, $J = 1$, Ar), 133.6 (d, $J = 2$, Ar), 133.5 (d, $J = 1$, Ar), 131.9 (d, $J = 30$, Ar), 131.5 (d, $J = 30$, Ar), 131.4 (d, $J = 2$, Ar), 131.3 (d, $J = 2$, Ar), 130.8 (d, $J = 2$, Ar), 130.6 (d, $J = 2$, Ar), 130.3 (Ar), 130.2 (Ar), 129.2 (d, $J = 4$), 129.1 (d, $J = 4$), 128.6 (d, $J = 7$), 128.5 (d, $J = 7$), 128.0 (d, $J = 2$), 127.4 (d, $J =$

9, Ar), 45.1 (dd, $J = 36$, 10, CH_2, *i*-Bu), 31.3−30.9 (m, CH_2), 29.6−29.3 (m, CH_2), 25.4 (d, $J = 8$, CH_3, *i*-Bu), 25.0 (CH, *i*-Bu), 27.9 (d, $J = 7$, CH_3, *i*-Bu), −1.7 (dd, $J = 80$, 6, Pt−Me).

Decomposition of 6 in the Presence of H_2O. A bright yellow solution of **6** (15 mg, 0.019 mmol) in toluene (0.5 mL) was transferred into an NMR tube, which was fitted with a septum, under N_2. H_2O (1 μL, 0.02 mol) was added via a microliter syringe, and the mixture was monitored by ^{31}P NMR spectroscopy. After 2 weeks, the solution turned colorless, colorless crystals (presumably **8**) formed on the walls of the NMR tube, and **12** was observed by ^{31}P NMR spectroscopy.

Decomposition of 6 in the Presence of H_2O and Air. A bright yellow solution of **6** (15 mg, 0.019 mmol) in toluene (0.5 mL) was transferred into an NMR tube. H_2O (1 μL, 0.02 mol) was added via a microliter syringe. The tube was left uncapped in the air, and the mixture was monitored by ^{31}P NMR spectroscopy. After 1 day, the solution became pale yellow and complexes **12** and **6** were observed. After 3 days, the solution turned colorless, and **12** was the only species observed by ^{31}P NMR. White flakes formed on the walls of the NMR tube; they turned into white crystals after 2 weeks. The solution was removed from the NMR tube; the crystals on the walls were washed with toluene, dissolved in $CDCl_3$, and shown, by ^{31}P NMR spectroscopy, to contain cation **8**. Two other peaks were also observed at 26.9 and 26.7 ppm. The toluene solution was mixed with the toluene washings, and the solvent was removed under vacuum. The white residue was redissolved in $CDCl_3$, and ^{31}P NMR spectroscopy showed that it was **12.** An additional peak at 33.8 ppm was also observed.

Decomposition of a Mixture of Pt(dppe)(Me)(PPh(*i*-Bu)) (6) and Pt(dppe)(Me)(P(O)Ph(*i*-Bu)) (12). A solution of **6** (39 mg, 0.05 mmol) in toluene (0.2 mL) was mixed with a solution of **12** (40 mg, 0.05 mmol) in toluene (0.3 mL). The mixture was transferred to an NMR tube, which was stored in a glovebox and monitored by ^{31}P NMR spectroscopy. After 10 days, the main components of the solution were **6** and **12**, but a small amount of cation **8**, along with several new peaks (δ 31.7, 29.6, 19.7, −11.6), was observed. After 2 months, a considerable amount of white precipitate had formed, and white crystals grew on the walls of the NMR tube. The intensity of the new peaks increased, and other new peaks were observed (δ −34.1, −34.5, −39.7 broad). The solution was decanted. The crystals on the walls of the NMR tube were dissolved in CH_2Cl_2; ^{31}P NMR spectroscopy showed that they were a mixture of cation **8** and **12**.

Acknowledgment. We thank the National Science Foundation for support and Cytec Canada for gifts of phosphines.

Supporting Information Available: Text and tables giving details of additional experiments on the formation of **8** from **6** and details of the crystallographic studies; crystallographic data are also given as CIF files. This material is available free of charge via the Internet at http://pubs.acs.org.

OM050149P